

# Comparative Study on Graphene-based Artificial Magnetic Conductor (AMC)

X.-C. Wang, W.-Y. Li, W.-S. Zhao, J. Hu,  
Y.-Y. Xu, and Q.-S. Huang

Centre for Opt. & EM Research, Zhejiang Provincial Key Lab for Sensing Technologies  
State Key Lab of MOI, Zhejiang University, Hangzhou 310058, China

**Abstract**— In this work, the graphene is employed to form artificial magnetic conductor (AMC). It is demonstrated that both the resonance frequency and bandwidth of graphene-based AMC can be tuned by varying the external electric field. Additionally, the graphene-based AMC with different geometries are examined and compared.

## 1. INTRODUCTION

Over the past several years, artificial magnetic conductor (AMC) has attracted much attention due to its ability in suppressing the surface wave and realizing the low-profile antennas. The AMC ground plane has a perfect magnetic conductor characteristic over a certain frequency range, i.e., the so-called AMC operation bandwidth, which is defined in the frequency range corresponding to the reflection phases between  $+90^\circ$  and  $-90^\circ$ . The main drawback of AMC ground plane is its relatively narrow bandwidth compared to the ultra-wide bandwidth (UWB) antenna. Typically, there are two ways to broaden the bandwidth of the AMC: 1) Modify the AMC structure such as using via holes or adopting multilayer FSS over a grounded substrate; and 2) insert varactor diodes between the AMC units [1, 2]. However, these methods become tough at very high frequencies (for example THz) due to the complex manufacturing process.

Recently, tunable THz devices based on graphene are successfully developed by using the variable surface conductivity of graphene under different applied voltages. In this work, the tunability of graphene-based AMC is proposed and demonstrated. By varying the chemical potential, the equivalent capacitance of the graphene-based AMC can be dramatically tuned, and the resonance frequency shifts subsequently.

## 2. GRAPHENE-BASED AMC

Figure 1(a) shows the graphene-based AMC unit, and the surface impedance can be characterized as a capacitor. The equivalent circuit model is shown in Fig. 1(b).

### 2.1. Analytical Modeling

The reflection phase  $R$  for graphene-based AMC with square patches is obtained by [3]

$$R = \frac{Z_s - \eta_0}{Z_s + \eta_0} \quad (1)$$

where  $\eta_0 (= 377 \Omega)$  is the intrinsic impedance of free-space, and  $Z_s$  is the total surface impedance, which can be calculated by (see Fig. 1(b))

$$Z_s = \left( \frac{1}{Z_d} + \frac{1}{Z_g} \right)^{-1} \quad (2)$$

where  $Z_d$  and  $Z_g$  are the impedances of grounded substrate and patch array, respectively [3, 4]

$$Z_d = j \frac{\eta_0}{\sqrt{\epsilon_r}} \tan(k_d t) = j\omega L_d(\omega) \quad (3a)$$

$$Z_g^{\omega\tau \gg 1} = j \left( \frac{D}{D-g} \frac{\omega\tau}{\sigma_0(\mu_c)} - \frac{1}{\omega C_{eff}} \right) = \frac{1}{j\omega C_g(\omega)} \quad (3b)$$

$$\sigma_0(\mu_c) = \frac{e^2 k_B T \tau}{\pi \hbar^2} \left[ \frac{\mu_c}{k_B T} + 2 \ln \left( 1 + e^{-\mu_c/k_B T} \right) \right] \quad (3c)$$

where  $D$  is the patch width,  $g$  is the patch gap,  $\epsilon_r$  is the relative permittivity of the substrate,  $t$  is the substrate thickness,  $k_B$  is the Boltzmann's constant,  $h$  is the reduced Planck's constant,  $T$  is the temperature,  $\tau$  and  $\mu_c$  are the relaxation time and chemical potential of the graphene sheet, respectively. The comparison between the analytical and simulated results is plotted in Fig. 2, and good agreement can be observed. Here,  $D = 8 \mu\text{m}$ ,  $g = 1 \mu\text{m}$ ,  $t = 8 \mu\text{m}$ , and the substrate is selected as  $\text{SiO}_2$ . By changing  $\mu_c$  from 0.4 eV to 1 eV (see Fig. 3), the resonance frequency can be tuned from 1.88 THz to 2.67 THz, and a wide bandwidth of 50% can be achieved. It is also found that the graphene-based AMC will be more reflective as  $\mu_c$  increases.

The performance of AMC ground plane will be affected in the case of oblique incidence, as shown in Fig. 4(a). With the increase of incident wave angle  $\theta$ , the resonance frequency increases, while the bandwidth decreases, as shown in Fig. 4(b). Also, the impact of  $\theta$  becomes more significant as it increases.

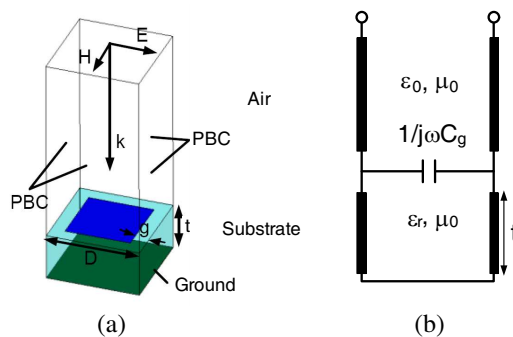


Figure 1: (a) Schematic of the AMC unit, and (b) its equivalent circuit model.

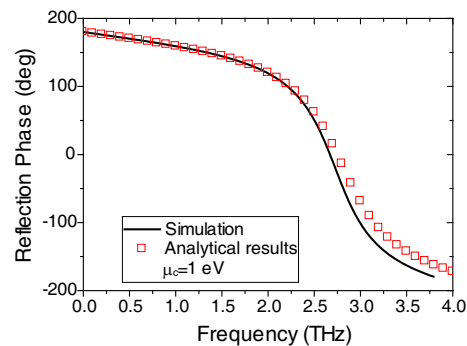


Figure 2: Comparison between analytical and simulated results for graphene-based AMC with square patches.

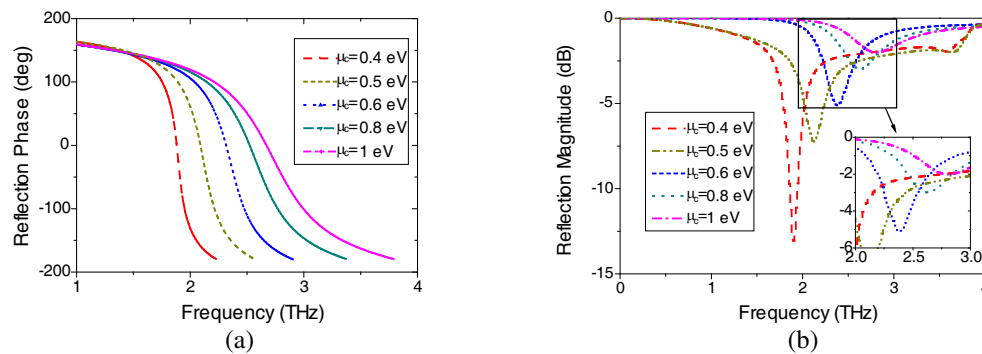


Figure 3: The reflection of the graphene-based AMC with different chemical potentials. (a) Phase; (b) Magnitude.

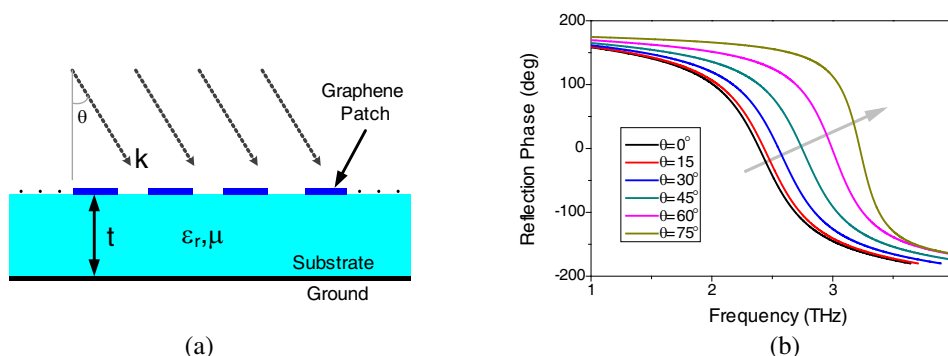


Figure 4: (a) Schematic view and (b) reflection phase of graphene-based AMC. The angle of incident wave is denoted by  $\theta$ .

## 2.2. Parametric Study

The impacts of  $D$ ,  $g$ ,  $t$ , and  $\epsilon_r$  are investigated for graphene-based AMC ground plane, as shown in Figs. 5(a)–(d). Both the bandwidth and resonance frequency of the graphene-based AMC can be decreased by increasing either  $D$  or  $\epsilon_r$ , while  $g$  has an opposite effect. By employing thicker substrate, the resonance frequency decreases but the bandwidth increases greatly. Nevertheless, it is impossible to thicken the substrate unlimitedly since the grounded substrate will not exhibit an inductor when  $t$  becomes larger than  $\lambda/4$ .

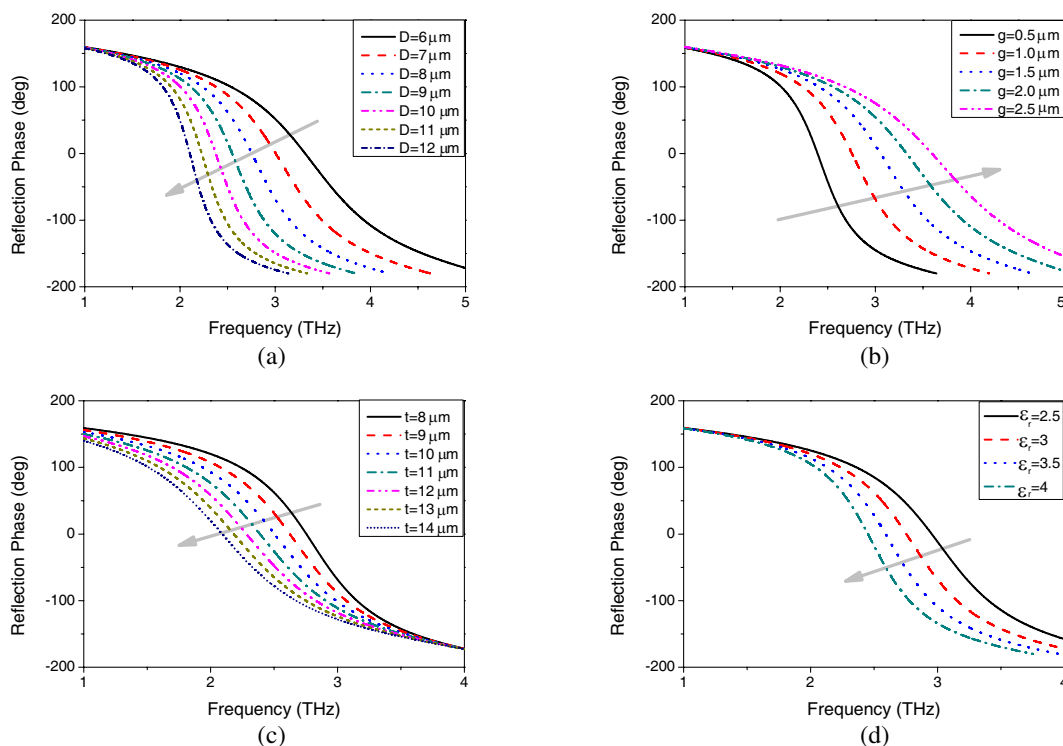


Figure 5: Parametric study of graphene-based AMC with (a)  $D$ , (b)  $g$ , (c)  $t$ , and (d)  $\epsilon_r$ , respectively.

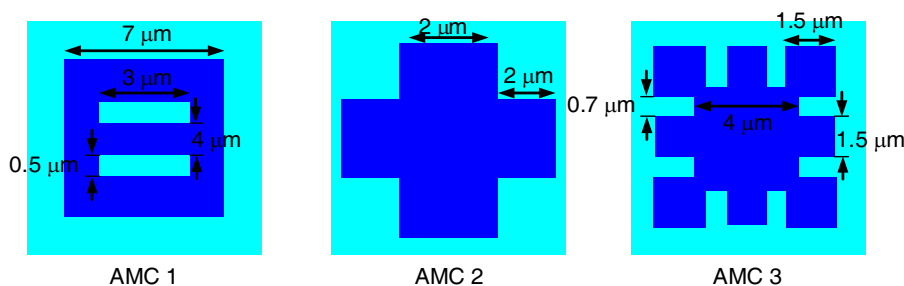


Figure 6: Schematic of different geometric shapes for graphene-based AMC.

## 3. DIFFERENT GEOMETRIC SHAPES

Various kinds of geometric shapes are studied in this section (see Fig. 6), and their reflection phases under different chemical potentials are plotted in Figs. 7(a)–(c). It is shown that the AMC 2 exhibits larger bandwidth while the AMC 1 shows a better tunability, as shown in Fig. 7(d). This phenomenon is because that the tunability of AMC ground plane is mainly determined by the equivalent capacitance contributed by the structure. From (3b), it is found that a larger  $C_{eff}$  means that the reactance contributed by graphene dominates thus a better tunability can be attained.

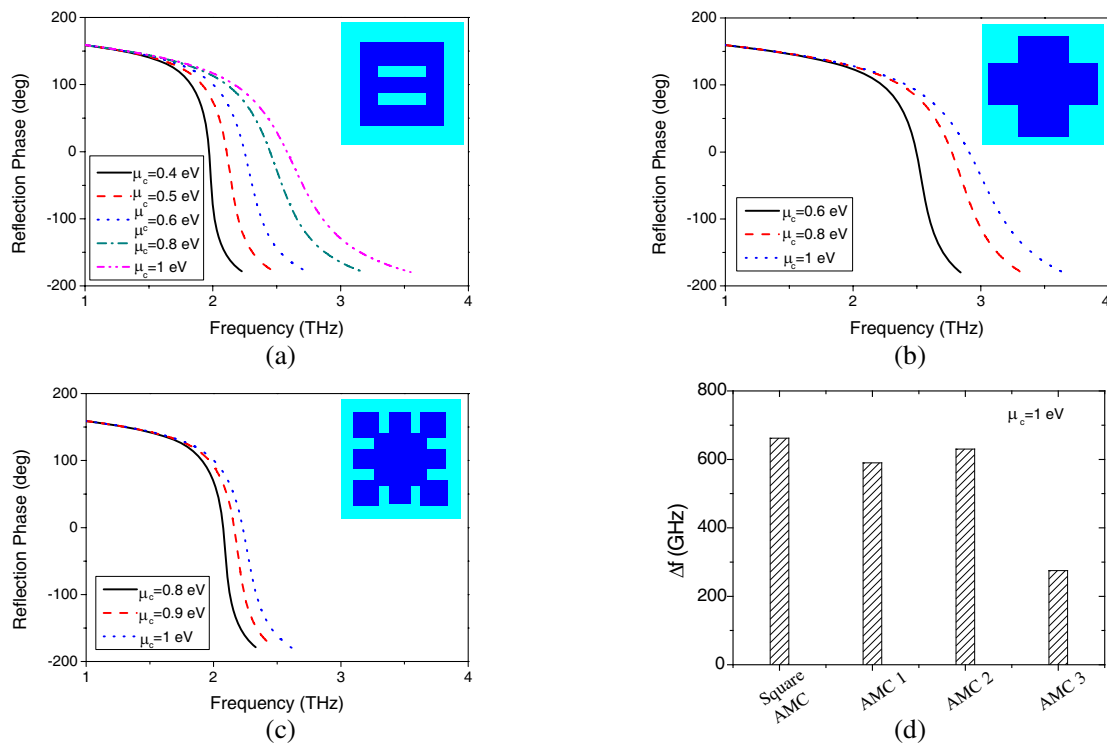


Figure 7: (a)–(c) The reflection phases of graphene-based AMC with different geometric shapes, and (d) comparison of frequency range  $\Delta f$ .

#### 4. CONCLUSION

In this work, a tunable graphene-based AMC is proposed and demonstrated. It is shown that both the resonance frequency and bandwidth increases with the increase of applied voltage. Parametric study is also conducted to find the influence of the geometries on the AMC performance. Finally, the bandwidth and tunability of different AMC shapes are examined and compared.

#### ACKNOWLEDGMENT

This research was supported by the Program of Zhejiang Leading Team of Science and Technology Innovation.

#### REFERENCES

1. Veysi, M. and M. Shafee, "EBG frequency response tuning using an adjustable air-gap," *Progress In Electromagnetics Research Letters*, Vol. 19, 31–39, 2010.
2. Costa, F., S. Talarico, A. Monorchio, and M. F. Valeri, "An active AMC ground plane for tunable low-profile antenna," *Int. Symp. Antennas Propag.*, 1–4, San Diego, CA, 2008.
3. Tretyakov, S., *Analytical Modeling in Applied Electromagnetics*, Artech House, Inc., 2003.
4. Hanson, G. W., "Dyadic Green's functions for an anisotropic non-local model of biased graphene," *IEEE Trans. on Antennas Propag.*, Vol. 56, No. 3, 747–757, 2008.